JOURNAL OF GEOPHYSICAL RESEARCH, VOL. 106, NO. C8, PAGES 16,825–16,840, AUGUST 15, 2001

Validation of two algorithms to retrieve ocean wave spectra from ERS synthetic aperture radar

A. C. Voorrips[1]
Royal Netherlands Meteorological Institute, De Bilt, The Netherlands

C. Mastenbroek[2]
Argoss, Vollenhove, The Netherlands

B. Hansen
European Centre for Medium-Range Weather Forecasts, Reading, United Kingdom

Abstract. Wave spectra that are retrieved from ERS-1/2 synthetic aperture radar (SAR) wave mode observations with two different algorithms are validated against 6 years of buoy observations. The Max-Planck Institut für Meteorologie (MPIM) algorithm, which runs operationally at the European Centre for Medium-Range Weather Forecasts (ECMWF), is found to deteriorate the quality of the WAM spectrum which is used as a first guess. The Semi-Parametric Retrieval Algorithm (SPRA) does not use a first-guess spectrum. For wavelengths which are observed by the SAR, it has a skill comparable to WAM. Several causes for the poor performance of the MPIM scheme are suggested. First, despite the fact that the SAR generally does not resolve the wind sea peak, the MPIM scheme allows for independent adjustment of its energy and peak frequency. Second, by using the quasi-linear approximation in the inversion, the scheme is inclined to interpret the SAR signal at low wave numbers as swell, whereas often it is generated by waves at higher wave numbers via nonlinearities in the SAR mapping. Third, the MPIM scheme is not able to adjust the spectral width of wave systems. The SPRA scheme retrieves swell information only up to a 180° directional ambiguity, and the SPRA retrievals often contain a spectral gap between the shortest waves observed by the SAR and the parameterized wind sea. In conclusion, the retrieval scheme performing best is the SPRA scheme, which has an accuracy comparable to WAM model output for the longer-swell waves.

1. Introduction

Satellite synthetic aperture radar (SAR) is the only source of spectral wave measurements with a global coverage. Since the launch of ERS-1 in 1991, the European Remote Sensing satellites ERS-1 and ERS-2 have supplied a continuous stream of SAR observations of the sea surface. Operating in the so-called wave mode, ERS-1 and ERS-2 acquire small, 5 by 10 km images every 200 km along their tracks. The 1500 imagettes that are collected daily contain valuable information on the spectral and angular distribution of the energy of ocean surface waves, in particular, of the swell waves longer than 200 m. Important potential applications of this unique data set include the computation of global wave statistics for climate atlases and the improvement of sea state analyses by operational wave models.

However, it is not straightforward to derive the two-dimensional wave spectrum from the SAR observation. The orbital motions of the surface waves cause a Doppler shift in the reflected radar signal. As a SAR interprets such Doppler shifts as displacements in the azimuthal direction, the image of the ocean surface gets distorted. *Hasselmann and Hasselmann* [1991] (hereinafter referred to as HH91) and *Krogstad* [1992] derived a closed expression for the "forward mapping" of

[1]Now at Cap Gemini Ernst & Young, Utrecht, The Netherlands

[2]Now at Topicus, Deventer, The Netherlands

Paper number 1999JC000156.
0148-0227/01/1999JC000156$09.00

a wave spectrum onto the observed SAR spectrum (the autospectrum of the SAR image). Owing to the interference of the orbital motions with the SAR image formation, this mapping is nonlinear in the ocean wave spectrum. HH91 show that the orbital velocities of all wave components, including the ones not resolved by the SAR, cause a degradation of the azimuthal resolution. The nonlinearity of the SAR mapping also causes energy of short-wave components to be transferred to the long-wave part of the SAR spectrum. These two effects imply that the inversion of the SAR-to-wave mapping relations has no unique solution. To interpret a SAR image spectrum in terms of an ocean wave spectrum, assumptions have to be made on the spectral level of wave components that are not resolved by the SAR. In addition to the nonlinear effects, the autospectrum of the "frozen" SAR image only allows the wave propagation direction to be determined up to a 180° ambiguity.

In order to retrieve an ocean wave spectrum from an observed SAR spectrum, additional information is necessary. Various inversion methods can be formulated, differing in the kind of additional information (model spectra, other observations) that is used, in the relative weight that is given to the various data and in the search strategy for the optimal solution. The performance of any of these methods can only be judged by comparison of their results against independent information, either from collocated in situ or satellite measurements or from model predictions.

Several different retrieval algorithms have been developed over the past decade. The first one, developed at the Max-Planck Institut für Meteorologie (MPIM) in Hamburg, was published by HH91 (an adapted version is described by *Hasselmann et al.* [1996]). The basic idea of this algorithm is to start with a wave spectrum from the numerical wave model WAM (*WAMDI Group, 1988* ; *Komen et al.*, 1994) and to change this wave spectrum iteratively so that its SAR image spectrum matches the observed SAR spectrum. *Krogstad et al.* [1994] employ a similar approach but simplified the iteration procedure by approximating the full nonlinear SAR mapping by the quasi-linear version. The quasi-linear mapping (HH91) ignores the nonlinear transfer of energy between different wave components but does account for the degradation of the azimuthal resolution. In a third inversion strategy, called Semi-Parametric Retrieval Algorithm (SPRA), the SAR observation is combined with a wind measurement from the scatterometer [*Mastenbroek and de Valk*, 2000]. Apart from the parameterized wind sea, this method only yields the wave components resolved by the SAR, and it is not able to resolve the 180° ambiguity in the propagation direction of the swell.

Very little is known about the relative skill of the different retrieval algorithms. In the work of *Bauer and Heimbach* [1999] the significant wave heights retrieved with the MPIM scheme are compared with altimeter measurements. They find that the significant wave heights of the Topex altimeter and the MPIM ERS-1 SAR retrievals agree "remarkably well." However, it is difficult to relate the reported validation results to other sources of spectral wave data. A second problem with the validation of only one integrated parameter like the significant wave height is that it gives very limited information on the spectral capabilities of the retrieval.

Another very indirect way to assess the performance of a SAR inversion scheme is through assimilation of the SAR data into a wave model, followed by a validation of the model results with and without assimilation against independent data. Using the MPIM inversion scheme for SAR data, *Dunlap et al.* [1998] performed an assimilation experiment in the North Atlantic, but the wave height analysis did not improve convincingly when compared with buoy data or altimeter wave height data. In the work of *Hasselmann et al.* [1997] and *Bauer et al.* [1997] some positive impact of SAR data assimilation was reported, but only in a comparison against the SAR wave spectra themselves and hence without reference to independent data. *Breivik et al.* [1998], finally, conducted a SAR assimilation experiment in the northeast Atlantic by using the inversion method of *Krogstad et al.* [1994]. On average, the results showed neutral impact of the assimilation when compared with either ERS-2 altimeter data or two measurement buoys. In some extreme cases a positive impact was found, but the statistical significance of these results is not clear. In summary, assimilation experiments conducted until now do not conclusively show that wave analyses and forecasts improve owing to SAR assimilation. From these studies alone, it cannot be decided whether this is due to SAR measurement errors, the retrieval method, imperfections in the assimilation methods, or simply the limited coverage of the SAR observations.

In the present study the MPIM and the SPRA scheme are validated simultaneously to allow for an appraisal of the two different strategies. The retrieved wave spectra are compared with energy density spectra from 39 buoys located in various ocean basins. As a reference, spectra from the WAM model that runs operationally at the European Centre for Medium-Range Weather Forecasts (ECMWF) are included in the validation. In section 2 a short description of the methods is given, including a summary of the available validation results. Section 3 describes the data sets used for the comparison. Validation results over a 5-year period are given in section 4. We discuss the results in section 5 with the help of a few examples of the inversion. Finally, we summarize the main conclusions in section 6.

2. Retrieval Schemes

2.1. MPIM Method

The original MPIM scheme (HH91) was the first SAR-to-wave retrieval method ever. It has been implemented at various research institutes and is running operationally at ECMWF. The scheme uses a first-guess spectrum from a wave model to fill in the missing information in the SAR spectrum. It finds the "retrieved" or "best guess" wave spectrum by minimizing a cost function which consists of two terms. One term penalizes the difference between the observed SAR spectrum and the SAR spectrum corresponding to the trial wave spectrum, and the other term penalizes the difference between the first-guess wave spectrum and the trial wave spectrum. The SAR spectrum of the trial wave spectrum is calculated with the full nonlinear mapping relation. In contrast, a quasi-linear approximation of the wave-to-SAR mapping relation is used for the calculation of the gradient of the cost function, which is necessary to obtain a search direction for minimization.

An adaptation to the original scheme was published by *Hasselmann et al.* [1996]. It differs in two important ways from the original scheme. First, a term is added in the cost function which penalizes the difference in azimuthal cutoff wave number of the observed and trial SAR spectrum. To minimize this term, the entire wave spectrum can be rescaled by a constant factor. Second, an extra iteration loop is added to the minimization procedure. After minimization of the cost by the old, "inner" iteration, both the first-guess and the "inverted" spectrum are separated into individual wave systems by using a partitioning technique. Then the first-guess wave systems are shifted and rescaled to match the mean parameters of the wave systems in the "inverted" spectrum. This new spectrum is used as a new first guess for the next iteration, and so forth. The result of the extra iteration loop is that the transition from the observed to the unobserved parts of the spectrum is smoother and that the resulting wave spectrum is less dependent on the initial first-guess spectrum.

The MPIM scheme which is used in the present comparison is the adapted scheme, with minor changes to the version described in the references given above. The main change was in the calibration of the SAR spectrum, i.e., the calculation of the normalized spectrum from the uncalibrated wave mode product using an estimate of the clutter noise (HH91). The calibration factor was enhanced by 1.7% (P. Heimbach, personal communication, 1998), yielding slightly larger wave heights.

In the work of *Heimbach et al.* [1998] the performance MPIM retrieval in combination with the operational ECMWF WAM model is assessed. It is reported that about a quarter of the SAR wave observations are rejected: in 15% of those cases no proper solution is found, and in 10% the wave height was considered to be too low. On the basis of a 3-year global data set it is concluded that the MPIM scheme on average overestimates the wave height with respect to WAM, especially for cases characterized by low swell. *Dunlap et al.* [1998], who also use a version of the MPIM scheme, report a 10–12% overestimation of the significant wave height. *Bauer and Heimbach* [1999] present a comparison of the significant wave height retrieved with the MPIM scheme with two altimeters (ERS-1 and Topex/Poseidon) for the year 1994. Using a relatively narrow collocation window of 60 km and 1 hour, they find an uncorrelated RMS error of 0.50 m between the SAR retrievals and the data from the Topex altimeter. It is difficult to assess the extent to which the SAR has contributed to this skill, as no comparison is presented between the first-guess WAM spectra and the altimeter measurements. Using a different data set of only a single month (May 1993), *Bauer and Staabs* [1998] find an RMS error between WAM and Topex of 0.37 m, some 25% smaller than that found in the comparison between the MPIM retrievals and Topex by *Bauer and Heimbach* [1999]. The average wave height in both samples was almost equal (2.8 m). Even though coarser collocation criteria were used in the WAM-Topex validation (200 km and 3 hours), it is difficult to draw conclusions from this result owing to the difference in data sets that were used.

2.2. SPRA Method

The SPRA retrieval scheme [*Mastenbroek*, 1998; *Mastenbroek and de Valk*, 2000] was developed to allow inversion of the SAR spectrum without need of a first-guess wave spectrum. Instead, the collocated wind observation from the ERS scatterometer is used to construct a first guess of the high-frequency wave components. The method is based on the observation that the nonlinearity of the forward mapping relation is mainly caused by the high-frequency components (wind sea), which have the highest orbital velocities. The mapping of additional swell is nearly linear (that is, tangent linear to the nonlinear transformation of the wind sea). This leads to the following two-step approach:

- A cost function is minimized which penalizes the difference between the observed SAR spectrum and the SAR spectrum corresponding to a parametrized wind sea spectrum [*Donelan et al.*, 1985]. The tunable parameters for the wind sea spectrum are the stage of development, or "wave age," and the angle between the wind and the propagation direction of the wind waves. Initially, it is assumed that the wind sea is fully developed and that the wind waves propagate in the wind direction observed by the scatterometer. Using the full nonlinear forward mapping, the optimal values for the wave age and propagation direction are found by minimizing the difference between the observed and calculated SAR spectra.

- The swell is calculated from the residual spectrum, i.e., the difference between the observed SAR spectrum and the SAR spectrum of the estimated wind sea. In this step, the tangent linear transformation is used; so it can be carried out without iteration.

In some cases, the swell does have a significant contribution to the total orbital velocity and hence to the azimuthal cutoff. Therefore the procedure above is iterated once. A drawback of the method is that a 180° ambiguity in the wave propagation direction of the swell cannot be resolved. For this, additional information (e.g., from a wave model) will be required. It should be noted here that processing of the raw SAR signal in principle allows resolving the 180° ambiguity through cross-spectral methods [*Engen and Johnsen*, 1995]. Unfortunately, this information cannot be retrieved anymore from the standard form in which the ERS SAR measurements are distributed, the European Space Agency's SAR Wave Mode Product.

Mastenbroek and de Valk [2000] provide a comparison of the retrieved wave spectra with buoy data. For their validation they used a 5-year period (1993-1998) and data from 11 NOAA buoys located in the Pacific and the Atlantic. The significant wave height is underestimated by 0.30 m (on an average wave height in the sample of 2.5 m). This is attributed to the fact that the SPRA scheme misses swell components shorter than 100 m. The standard deviation is 0.70 m, which is comparable to the standard deviation of 0.75 m in the Topex-MPIM comparison of *Bauer and Heimbach* [1999]. The SPRA retrieval of the height of waves longer than 12 s has a negligible bias and a standard deviation of 0.40 m.

The MPIM and SPRA methods are different in many respects. One interesting aspect is the different constraints put on the retrieved wave spectrum. The SPRA scheme puts severe constraints on the wind sea part of the spectrum: this must be of the spectral form of *Donelan et al.* [1985]. The swell, on the other hand, can be matched bin by bin to the observed spectrum. In contrast, the MPIM method treats wind sea and swell on an equal footing: all wave systems can be shifted and rescaled to match the SAR spectrum, but on the other hand, the spectral form of every wave system is kept equal to the form of the corresponding first-guess wave system.

3. Data Sets

3.1. SAR and WAM Data

ERS SAR data have been obtained from ECMWF, together with the collocated wave spectra from the ECMWF global WAM model, which are necessary for the MPIM inversion. The collocated ERS scatterometer wind observations have been obtained from the Institut Français de Recherche pour l'Exploitation de la Mer (IFREMER). The data set starts in April 1993 (before that date, no WAM collocations were available) and ends in May 1998, when version 2 of the SAR Wave Mode Product was introduced.

Standard validation of the ECMWF WAM model against buoys shows the model to have a slight negative bias of about 0.2 to 0.3 m in its significant wave height [*Janssen et al.*, 1996]. The standard deviation of the significant wave height error in most regions is about 15% of the mean significant wave height. Near the east coast of the United States the scatter is larger

Table 1. List of the 39 Buoys Used in the Validation

Source[a]	Region	Buoy
NOAA	Pacific	46001, 46002, 46003, 46005, 46006, 46025, 46035, 46059
MEDS	Pacific	46004, 46184
NOAA	Hawaii	51001, 51002, 51003, 51004, 51026, 51028
NOAA	Atlantic	41001, 41002, 41004, 41006, 41010, 44004, 44005, 44008, 44011, 44014
MEDS	Atlantic	44137, 44139, 44141
RWS	North Sea	North Cormorant, AUK, K13
MHL	Australia	Byron Bay, Coffs Harbour, Crowdy Head, Sydney, Port Kembla, Batemans Bay, Eden

[a]NOAA, National Oceanic and Atmospheric Administration; MEDS, Canadian Marine Environmental Data Service; RWS, Rijkswaterstaat; MHL, Manly Hydraulics Laboratory

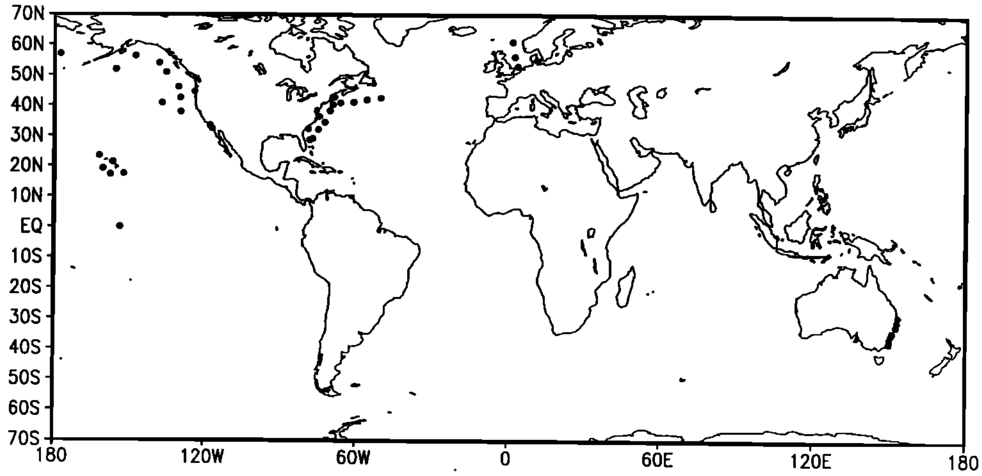

Figure 1. Locations of the 39 buoys used in the validation.

(25%), which is attributed to a larger spatial and temporal variability in the wave field due to strong currents.

3.2. Buoy Data

Wave spectra have been collected from 39 buoys along the U.S. and Canadian east and west coasts (National Oceanic and Atmospheric Administration (NOAA), Californian Coastal Data Information Program, and the Canadian Marine Environmental Data Service), near Hawaii (NOAA), in the North Sea (Dutch coastal authorities), and at the Australian east coast (Manly Hydraulics Laboratory). The buoys are listed in Table 1; their locations are depicted in Figure 1.

Most of these buoys are nondirectional: only frequency spectra are available. The few buoys that do measure directional information are mostly located close to the coast, which puts rather severe constraints on the SAR-buoy collocation criteria. Therefore we limit the validation of the spectra to the frequency spectra.

3.3. Collocation Criteria

To validate the SAR inversions against buoy data, we have chosen as collocation criteria a maximum time difference of 30 min and a maximum distance of 80 km between buoy and SAR measurement. These rather strict criteria were taken since some buoys are located rather close to the coast, which means that spatial gradients of wave parameters can be substantial. Furthermore, we selected only those SAR spectra for which both the collocated ERS scatterometer wind observations and WAM spectra were available, so that both schemes were able to carry out the inversion. Finally, the SPRA scheme has a quality control mechanism which rejects about 10% of the spectra owing to slicks and other nonwave features [*Mastenbroek and de Valk*, 2000]. We have removed those spectra also in the validation set for the MPIM scheme, first, because the quality control (QC) parameter of the MPIM scheme (see below) generally indicates low quality for these spectra as well and, second, because validation of MPIM retrievals for these spectra against buoy data shows much lower performance than average MPIM performance. A total of 1860 spectra matched the above criteria. The MPIM QC parameter was not used to further reject inversion results. Alternatively, the quality of the inversions is studied as a function of this parameter in section 4.2.3.

4. Validation Results 1993–1998

4.1. Significant Wave Height

Figure 2 shows scatter plots and statistics of buoy significant wave height (H_s) measurements versus WAM results and MPIM and SPRA retrievals. The NRSME is the RMS error normalized with the RMS significant wave height measured by the buoy.

Clearly, the WAM model results for this parameter are better than the SAR retrievals, both in terms of the bias and in terms of the standard deviation. Apparently, the MPIM scheme is not able to improve on the quality of the significant wave height of its first guess. The wave height of WAM is increased on average by 20% by the MPIM scheme, twice the value reported by *Dunlap et al.* [1998]. The scatter is some 25% lower in the WAM results than in the MPIM retrievals, which is consistent with the tentative conclusion that was drawn in section 2.1 on the basis of the comparison with the altimeter data. The standard deviation that we find, 0.75 m, is exactly equal to that reported by *Bauer and Heimbach* [1999].

The validation results for the significant wave height retrieved by the SPRA scheme are slightly worse than those reported by *Mastenbroek and de Valk* [2000]: both the negative bias and the standard deviation are somewhat larger. This may be caused by the larger max-

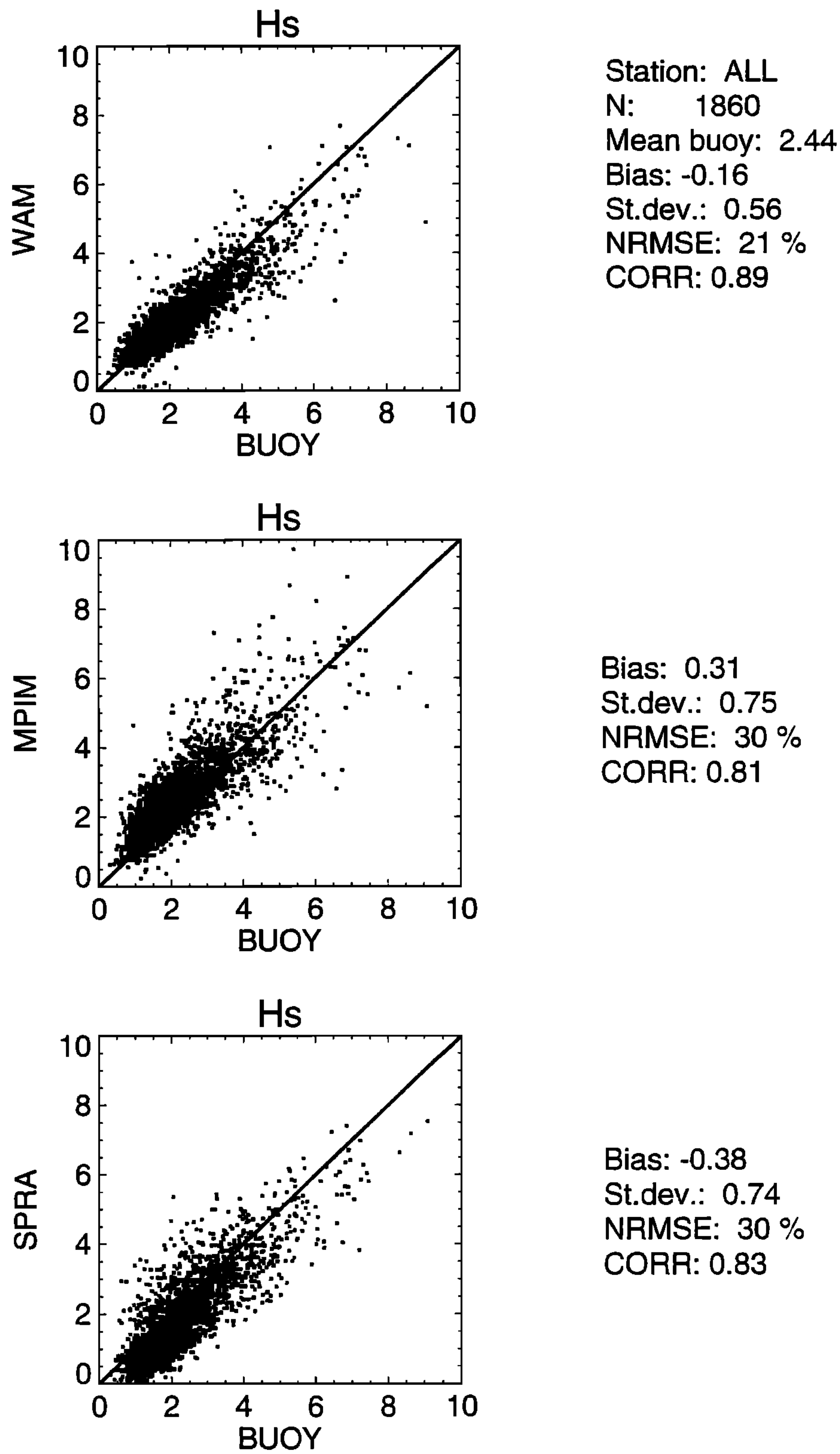

Figure 2. Scatter plots of H_s values from (top) WAM, (middle) MPIM retrieval and (bottom) SPRA retrieval versus buoy measurements.

imum collocation distance used in the study (80 km compared with 60 km), and by the fact that the present validation also includes buoys close to the shore, where the spatial variability may be larger than that on open ocean.

4.2. Low-Frequency Wave Height

4.2.1. Overall statistics. Owing to the degradation of the azimuthal resolution, waves shorter than a certain cutoff length traveling in the azimuthal direction are invisible to the SAR. For the ERS SAR, azimuth traveling waves shorter than approximately 150–200 m are visible only under light wind conditions. To do a bulk comparison, it is therefore useful to assess the quality of the SAR retrievals for waves longer than this threshold. For this purpose, we define the low-frequency wave height H_{12} in the following way:

$$H_{12} = 4\left\{\int_0^{1/12\mathrm{Hz}} F(f)df\right\}^{1/2}. \qquad (1)$$

This parameter incorporates the energy of all wave components with a period longer than 12 s, hence with a wavelength longer than 225 m in deep water.

Statistics for H_{12} are shown in Figure 3. As was the case with the significant wave height, we find that the WAM estimates compare better with the buoy data than the MPIM retrievals. The WAM results for the long-wave components are almost bias free; the MPIM retrievals have a bias of 0.35 m, which is more than 40% of the average value of H_{12}. The standard deviation of H_{12} retrieved by the MPIM scheme is 15% larger than that of its first guess. The quality of the MPIM retrievals is worse than the WAM results, even when we consider only the wave components resolved by the SAR.

The statistics of the SPRA scheme for the H_{12} parameter are comparable to those of the WAM model. As the SPRA does not use WAM spectra as an input, this means that it derived this skill from the SAR data. Hence the fact that the MPIM scheme deteriorates the quality of the WAM spectra cannot be blamed on the SAR observations, as the SPRA scheme extracts the H_{12} parameter from these observations with a skill comparable to that of WAM. Both WAM and SPRA have a tendency to underestimate high values of H_{12}: for the subset of cases larger than 2 m, both models have a negative bias of 0.50 m compared with the buoy measurements.

The most striking outcome of the above validation is that the MPIM scheme performs worse than WAM, despite the fact that the MPIM scheme uses WAM spectra as a first guess. In the next section we will try to analyze the reasons for this unexpected behavior. At this point, however, we will show that, even though the MPIM statistics are unfavorable with respect to those of WAM, the MPIM retrievals do actually contain independent information. Let us first assume the contrary, i.e., that the MPIM result is only the WAM result with noise added:

$$y_i = x_i + \varepsilon_i, \quad i = 1..N, \qquad (2)$$

where x_i is the error in the WAM estimate of H_{12}, y_i is the error in the MPIM estimate, ε_i is a random unbiased error with variance σ_ε^2, and $N = 1860$ is the sample size. In the above we ignore the systematic errors (bias), since they are not relevant for the discussion. The expected correlation between WAM and MPIM errors is then given by

$$r_{xy} = \frac{\langle xy \rangle}{\sigma_x \sigma_y} = \frac{\sigma_x}{\sigma_y}, \qquad (3)$$

where σ_x and σ_y are the standard deviations of the WAM and MPIM errors, respectively. In the second equality we have used (2) and the assumption that the noise ε_i is uncorrelated with the WAM error x_i. If we take the WAM and MPIM H_{12} residuals (i.e., differences between WAM/MPIM and buoy observation) as an approximation of the actual errors in the WAM/MPIM results, we can use (2) and the standard deviations listed in Figure 3 to compute an expected correlation coefficient of 0.86. In reality, the sample correlation coefficient computed directly from the residuals is much lower, only 0.42 (see Table 2). This shows that the MPIM scheme reduces the error of its WAM first guess and that a significant part of the error in the MPIM scheme is independent from that of WAM.

From the analysis above it is clear that the MPIM does extract information from the SAR, but the fact remains that the final error variance is larger than that from the WAM first guess. In order to quantify this further, we assume that the scheme reduces the WAM error with the help of SAR information but at the same time adds new noise due to deficiencies in the scheme:

$$y_i = f x_i + \varepsilon_i, \quad i = 1..N, \qquad (4)$$

where f is the factor with which the WAM error is reduced. Using the experimentally found standard deviations and correlation r_{xy}, we find $f = 0.49$ and $\sigma_\varepsilon = 0.46$ m. Hence the original WAM error is reduced by about 50%, but a random error is added which is on average slightly larger than the original WAM error.

In the above analysis we have assumed that the correlation between the WAM/MPIM errors is entirely due to these models. However, this correlation will partially be caused by errors in the buoy data. We can estimate this contribution by assuming that the actual errors of the SPRA retrieval and the WAM model are uncorrelated and that the correlation coefficient of 0.38 in table 2 is entirely due to errors in the buoy spectra. Un-

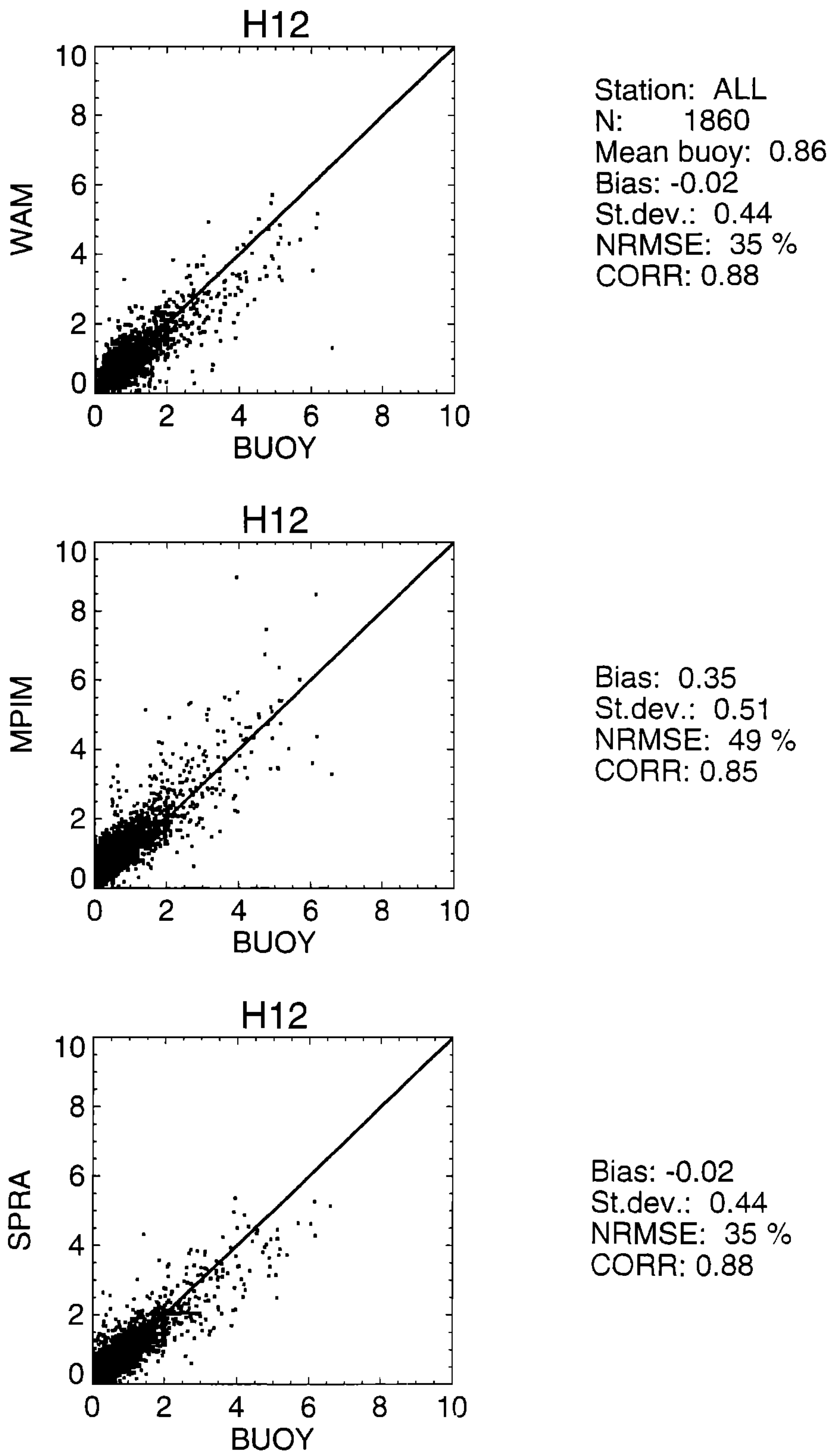

Figure 3. Same as Figure 2, but for H_{12}.

Table 2. Correlation Between Errors of the Three Models in the Parameter H_{12}

	MPIM	SPRA
WAM	0.42	0.38
MPIM		0.59

der that assumption the standard deviation in the buoy measurements of H_{12} is 0.27 m. Given this uncertainty in the buoy measurements, the standard deviation in both the WAM model and SPRA retrieval of H_{12} becomes 0.35 m, and that of the MPIM scheme is 0.43 m. If we correct for the contribution of the buoy error to the correlation between WAM and MPIM, we find that the error reduction coefficient of MPIM is $f = 0.17$. This confirms the claim of *Heimbach et al.* [1998] that the error in the MPIM retrieval is largely independent from that of the WAM first guess. However, the MPIM scheme adds its own random error to the retrieval with a magnitude that is on average larger than the error in the WAM first guess.

4.2.2. Dependence on region. In Table 3, the results for H_{12} have been stratified with respect to region. Although large regional variations occur in terms of average H_{12}, qualitatively the relative performance of the various schemes remains the same: SPRA and WAM perform about equally well, while the MPIM is of lower quality. Compared with the average value for H_{12}, the performance of all models is worst in the Atlantic, i.e., for the buoys along the east coast of the United States. In their validation of the WAM model, *Janssen et al.* [1996] also noticed this lack of skill in this region. An interesting point is that SPRA seems to perform slightly better than WAM in areas where low-frequency energy is a significant fraction of the total wave energy (Hawaii, northeastern Pacific), while in other regions WAM is performing better. A possible explanation is offered by the fact that the low-frequency part of the SAR spectrum is influenced by the high-frequency part through the nonlinear wave-to-SAR transformation: the larger the energy is in the unobserved part, the more difficult it is for the retrieval schemes to estimate the low-frequency part.

4.2.3. Dependence on MPIM quality parameter. In the statistics presented above, we have used all MPIM inversions. However, the MPIM scheme supplies a QC parameter which can be used to accept or reject part of the data. Table 4 stratifies the data with respect to this quality parameter. As can be seen, the inversions which are deemed "excellent" (QC = 0) or "acceptable" (QC = 1) by the scheme [see *Hasselmann et al.*, 1998, p. 32] correspond on average with wave spectra which have a relatively large amount of energy in the observed (low frequency) part of the spectrum. The MPIM performance in terms of bias or standard deviation, however, is not very sensitive to this parameter. On the other hand, there is a clear dependence of the WAM quality with respect to the QC parameter: going from QC = 2 (cost reduced with less than 50%) to QC = 0 (cost reduced with more than 90%), the WAM first-guess random error (standard deviation) increases from 0.38 to 0.53 m. Apparently, the amount by which the cost function decreases depends more on the quality of the first-guess spectrum than on the quality of the inversion, which again confirms that the MPIM inversion is relatively independent from the WAM first guess.

4.3. Spectral Wave Data

In order to investigate the performance of the schemes in more spectral detail, we calculated statistics in terms of narrowband wave heights, defined as

$$H_{T_1,T_2} = 4\left\{\int_{1/T_2}^{1/T_1} F(f)df\right\}^{1/2}, \tag{5}$$

where we chose wave period intervals $[T_1, T_2]$ of 2 s. Figure 4 shows histograms of bias, standard deviation, and normalized RMS error in terms of these "2-s" wave heights. Clearly, the performance of the retrievals and of WAM varies considerably with respect to wave pe-

Table 3. Statistics of H_{12} Retrievals and Model Results Versus Buoy Measurements for Various Regions.

Area	N	$\langle H_{12}\rangle$ Buoy, m	$\langle H_{12}\rangle/\langle H_s\rangle$ Buoy, %	Bias, m WAM	Bias, m MPIM	Bias, m SPRA	Standard Deviation Error, m WAM	Standard Deviation Error, m MPIM	Standard Deviation Error, m SPRA
All	1860	0.86	35	-0.02	0.35	-0.02	0.44	0.51	0.44
Pacific	612	1.31	45	-0.11	0.43	-0.02	0.52	0.61	0.50
Hawaii	449	0.93	39	0.09	0.30	-0.05	0.37	0.47	0.34
Atlantic	570	0.46	20	-0.06	0.28	0.05	0.41	0.43	0.44
North Sea	70	0.54	24	0.01	0.38	-0.01	0.30	0.49	0.34
Australia	159	0.50	32	0.12	0.41	0.09	0.29	0.42	0.36

Table 4. Statistics of H_{12} Retrievals and Model Results as a Function of the MPIM Quality Parameter[a]

QC Parameter	N	$\langle H_{12}\rangle$ Buoy, m	$\langle H_{12}\rangle/\langle H_s\rangle$ Buoy, %	Bias, m WAM	Bias, m MPIM	Bias, m SPRA	Standard Deviation Error, m WAM	Standard Deviation Error, m MPIM	Standard Deviation Error, m SPRA
All	1860	0.86	35	-0.02	0.35	-0.02	0.44	0.51	0.44
0	487	1.30	44	-0.10	0.37	0.01	0.53	0.54	0.46
1	556	0.94	37	-0.05	0.32	-0.05	0.46	0.58	0.47
2	40	0.51	24	0	0.38	0.07	0.38	0.52	0.44
3	534	0.69	30	0.05	0.38	-0.03	0.38	0.49	0.43
4	243	0.19	14	0.06	0.27	0.02	0.24	0.27	0.28

[a]QC = 0, cost reduced to less than 10% of the original value; QC = 1, cost reduced to 10-50%; QC = 2, cost reduced with less than 50%; QC = 3, no convergence in iteration; QC = 4, no azimuthal cut-off adjustment. QC = 0, 1 are usually accepted; QC = 2 is rejected, and QC = 3, 4 are deemed questionable

riod. WAM shows virtually no bias over the entire spectral range, while the standard deviation slowly increases with wave period. The MPIM method has a positive bias over the entire frequency range. The random error follows the same trend as the WAM random error but is somewhat higher than WAM for every wave period. The SPRA scheme, finally, has a significant negative bias and the largest random error in the unobserved part of the spectrum (wave periods smaller than 12 s). In the observed part, however, it performs better than the MPIM scheme and, for periods larger than 14 s even slightly better than WAM.

5. Discussion and Case Studies

A rather surprising result found in the previous section was that the MPIM scheme performs poorly in the retrieval of H_{12}, both in comparison with its first guess (WAM) and in comparison with the SPRA scheme. In this section we will analyze some specific cases to illustrate the kind of situations that pose problems for the MPIM scheme. However, the MPIM scheme is a complicated algorithm; so it is difficult to pinpoint the exact assumptions that fail. In the last case we will illustrate one of the limitations of the SPRA: its inability to retrieve information on (swell) waves not resolved by the SAR.

5.1. Relation Between Peak Frequency and Energy of Wind Sea

One of the differences between both the WAM model and the SPRA scheme on the one hand and the MPIM scheme on the other is that in the latter scheme the energy and the peak frequency of a wind sea are not related. In the WAM model (parameterized) physical mechanisms result in wind sea spectra in which the peak frequency decreases when the energy of the peak increases. By using a wind sea peak with a prescribed spectral shape, the SPRA algorithm more or less imposes this behavior. In the MPIM scheme the energy and the frequency of a wind sea peak are allowed to vary independently. As we will illustrate with the following example, the ERS SAR does not as a rule provide

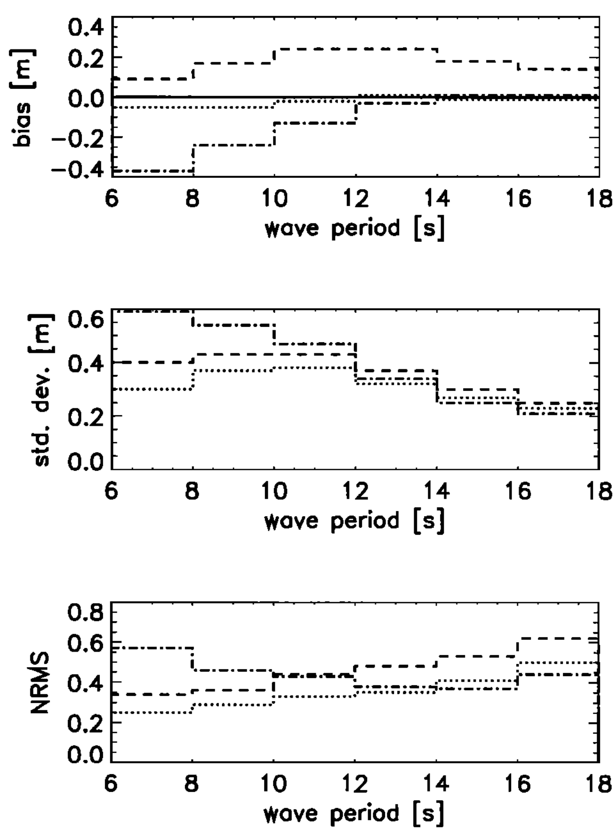

Figure 4. (Top) bias, (middle) standard deviation and (bottom) normalized RMS error (NRMS) of 2-s interval wave heights H_{T_1,T_2}, compared with corresponding buoy wave heights. NRMS error is defined as the RMS error divided by the RMS buoy value. Dotted line, WAM; dashed line, MPIM; dash-dotted line, SPRA scheme.

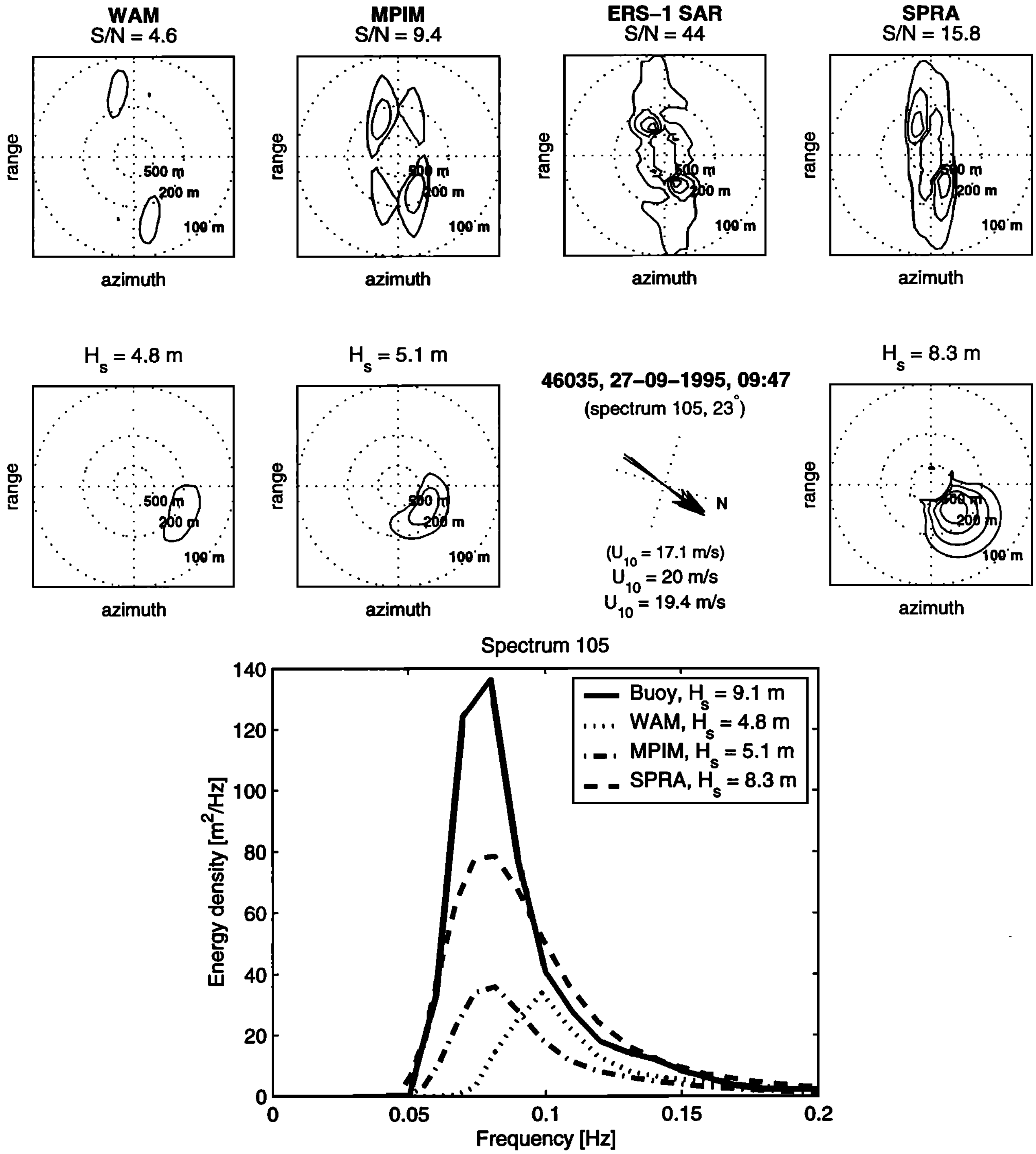

Figure 5. Illustration of an unrealistic wind sea peak from the MPIM retrieval. The upper panel row of plots shows SAR image spectra, and the second row (apart from the third plot) shows wave spectra, all spectra in the wave number domain with the x axis directed in the azimuth direction and the y axis in the range direction. Indicated are circles corresponding to 100-, 200, and 500-m wavelength. From left to right are shown the WAM wave spectrum (lower plot) and corresponding SAR spectrum (upper plot), the wave spectrum derived from the MPIM algorithm and its corresponding SAR spectrum, the SAR spectrum observed by ERS-1 (upper row), and the wave spectrum derived from the SPRA algorithm and its corresponding SAR spectrum. The plot woth the arrows on the second row indicates the wind speed and direction as predicted by the ECMWF model (first value, between brackets) and as measured by the scatterometer (second value) and the buoy (third value). The bottom figure shows the energy density spectrum as observed by buoy 46035 and those values obtained from the WAM model and the MPIM and SPRA retrieval algorithms. Solid line, buoy spectrum; dotted line, WAM spectrum; dashed-dotted line, MPIM spectrum; dashed line, SPRA spectrum.

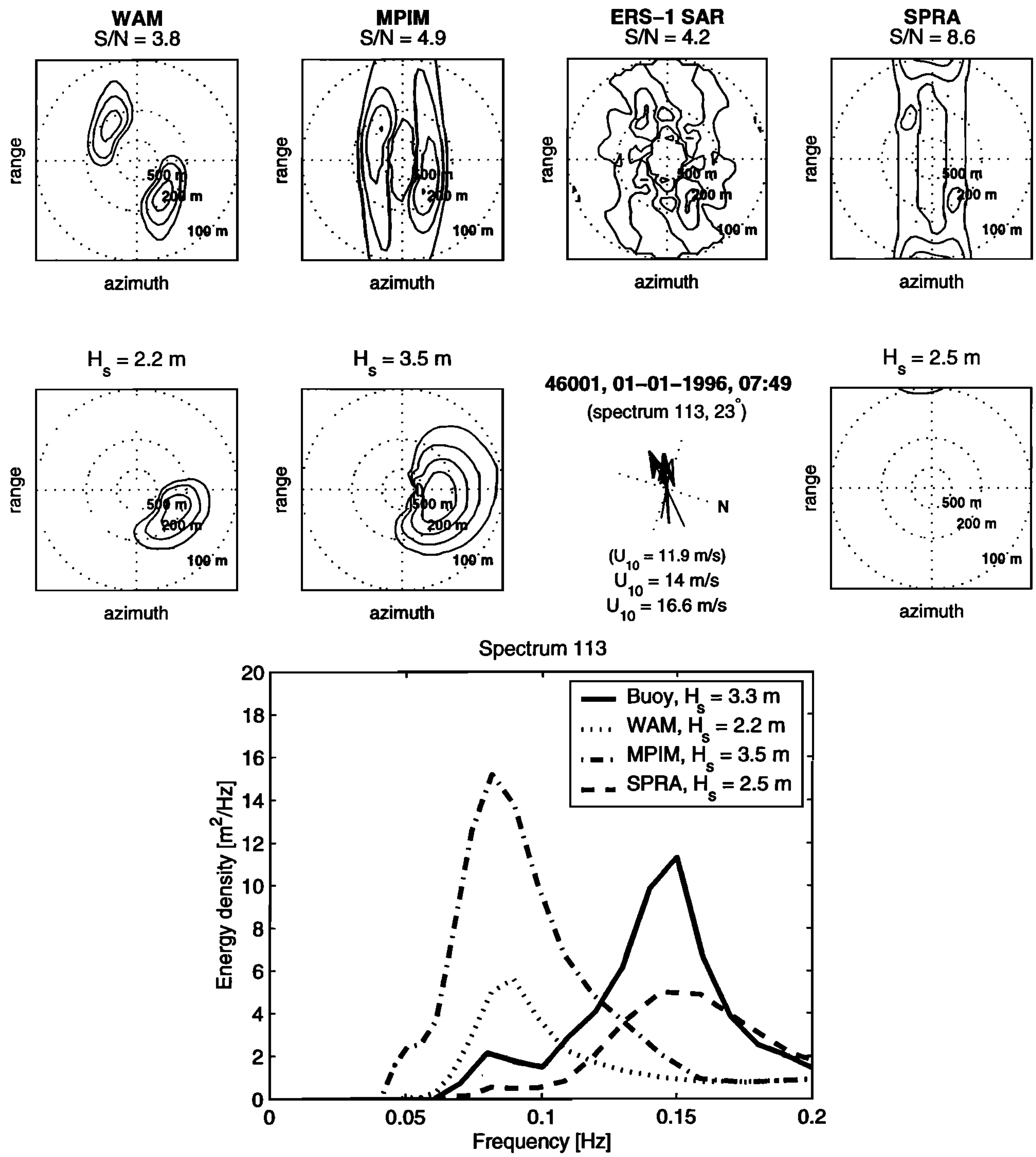

Figure 6. Noisy signal observed by the ERS-1 SAR (top row, third column) is interpreted differently by the MPIM and SPRA algorithms. The MPIM scheme enhances the swell peak that was already present in its first-guess WAM spectrum; the SPRA method attributes the signal to spillover from the wind sea peak just outside the domain directly accessible by the SAR. Meaning of plots: the same as in Figure 5.

enough information on the wind sea peak to handle this freedom properly.

Figure 5 shows a clear wind sea case, the buoy indicates that the wave spectrum is almost fully developed ($U_{10}/c_p \simeq 1$). WAM underestimates the wave height, partially owing to an underestimation of the wind (17.1 m/s ECMWF versus 20 m/s scatterometer, 19.4 m/s buoy). In accordance with the SAR observation, the MPIM scheme shifts the peak to a lower frequency. However, it does not increase the energy of

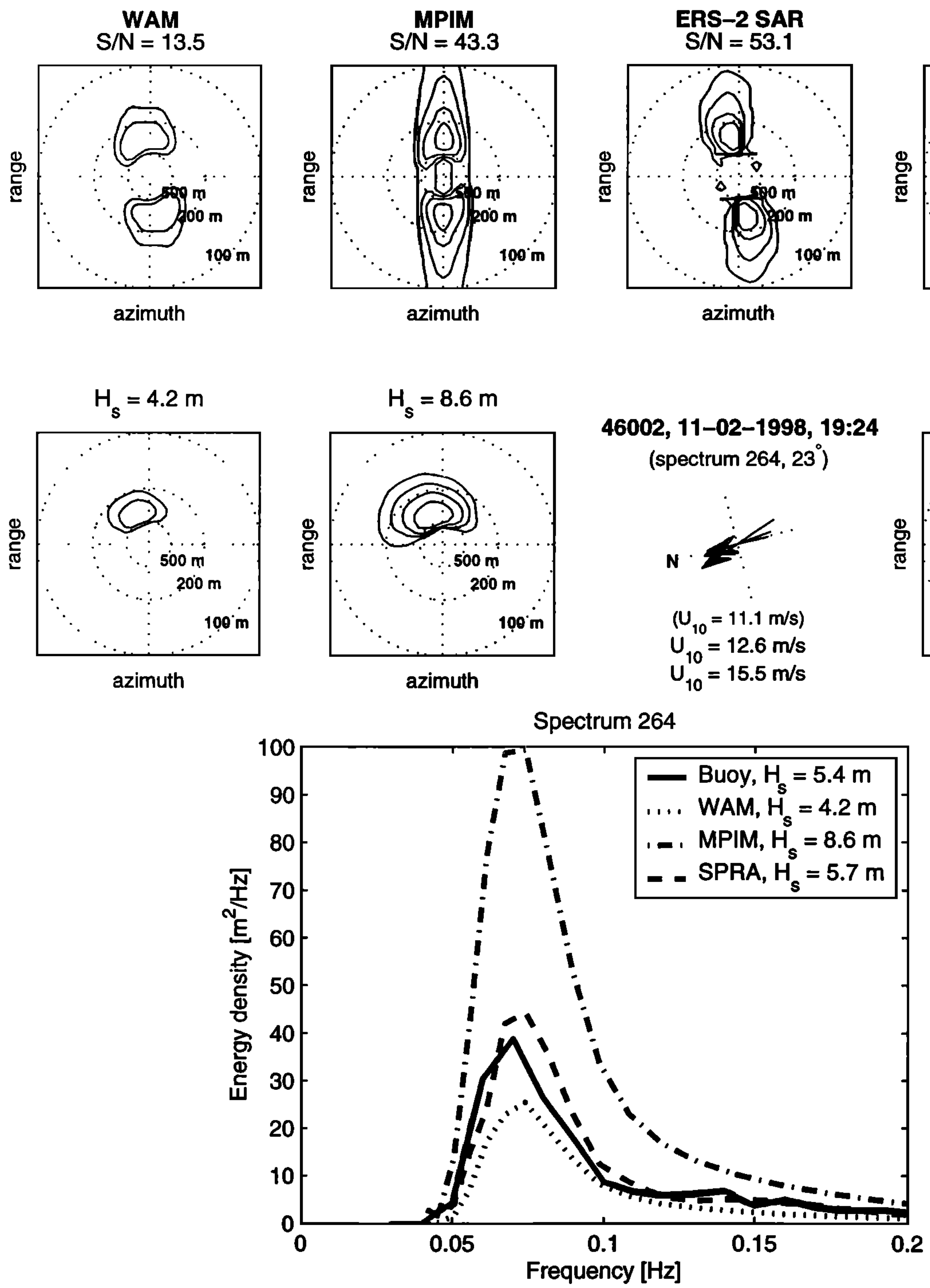

Figure 7. MPIM scheme matches the observed SAR signal by increasing the level of the relatively wide swell peak in the WAM spectrum, whereas the SPRA method assumes the peak to be much narrower. Meaning of plots: the same as in Figure 5.

the wind sea peak. The problem here is that this leads to an unrealistic spectrum: wind sea spectra generally have a semi-universal form which relates lower peak frequency to higher energy. The SPRA scheme imposes a prescribed spectral shape, and although this may not be perfect, its results correspond much better with the observed buoy spectra.

5.2. Nonlinearity in the SAR Mapping

Another potential problem with the MPIM scheme is the fact that mismatches with the observed SAR spectrum are mapped back to the wave spectrum with the inverse quasi-linear model of HH91. In the quasi-linear approximation the transfer of energy from high- to low-

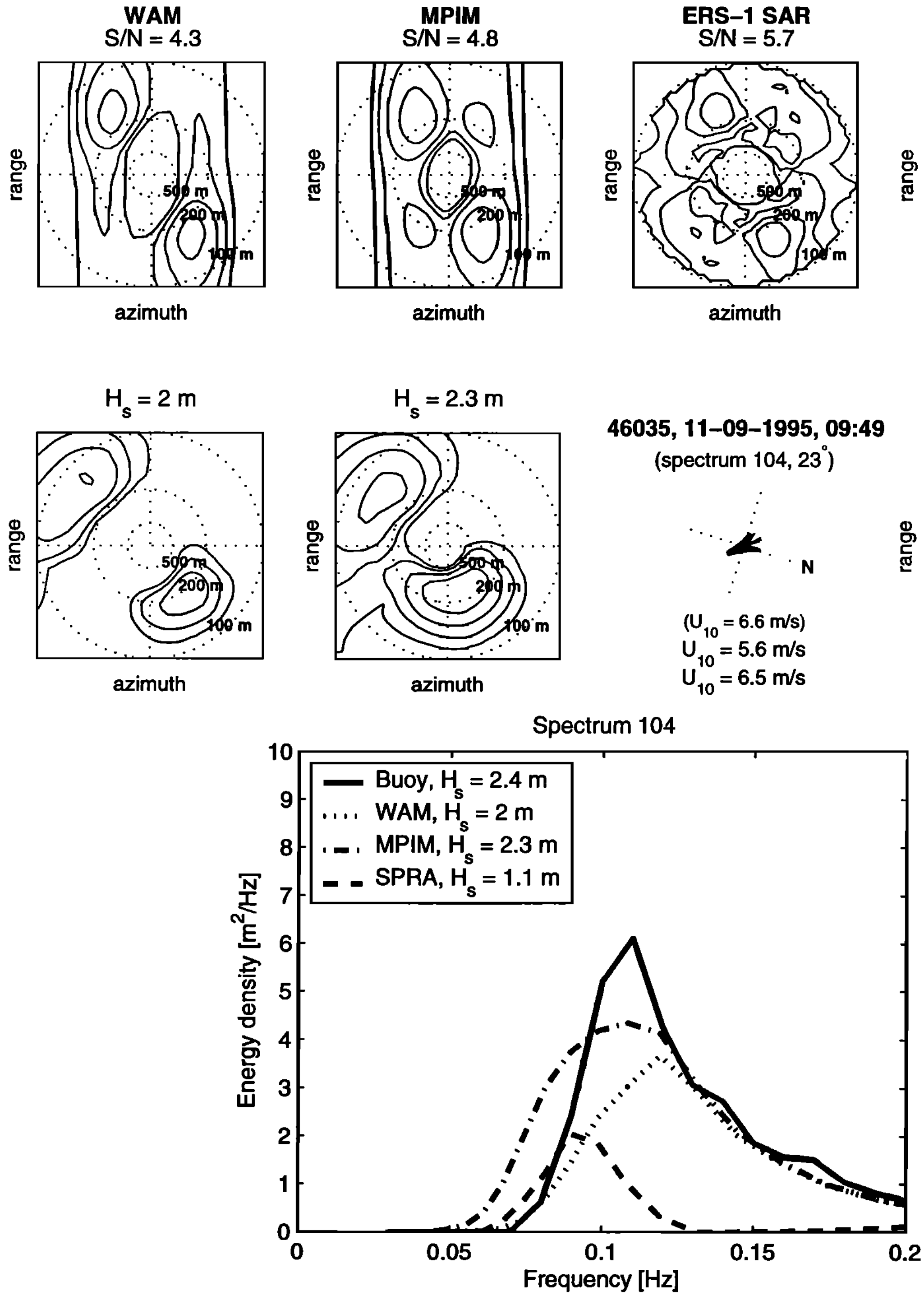

Figure 8. In light wind conditions, the SPRA method suffers from a large spectral gap between the shortest wave the SAR can resolve successfully (about 150 m, or 0.1 Hz, in practice), and the wind sea at the high-wave-number end of the spectrum. Meaning of plots: the same as in Figure 5.

azimuth wave numbers is ignored. In the case that the wind sea is underestimated by WAM, it is likely that the energy which this wind sea creates in the low-frequency part of the SAR spectrum (caused by the nonlinearity in the SAR mapping) is interpreted by the MPIM scheme as swell. Figure 6 shows an example of this. Again, the model wind (11.9 m/s) is lower than the observed wind (scatterometer, 14 m/s; buoy, 16.6 m/s), and the MPIM scheme tries to compensate for the missing energy in the SAR spectrum by adjusting a swell system, which actually was already overestimated in the WAM first guess. Note that in the SPRA case the low-azimuth wave number signal in the SAR observation is matched by energy that is transferred from the wind sea peak located at a higher wave number. This wind sea peak was not present to the same extent in the WAM first guess.

5.3. Spectral Width of WAM Peaks

A third point that might have to be improved in the MPIM scheme is the fact that in order to match the SAR spectrum, WAM first-guess partitions may be rotated and scaled, but that the spectral form (especially spectral width) is not allowed to vary. More often than not, SAR spectra calculated from the first-guess WAM spectra are less peaked than the SAR spectrum observed by the ERS satellite. Since the spectral width is not allowed to vary, the SAR spectrum corresponding with the retrieved wave spectrum often shows either a peak that is too low or a peak with the right maximum but which is too wide. An example of the latter is shown in Figure 7. Here the first-guess energy spectrum of WAM only slightly underestimates the collocated buoy spectrum. However, the peak of its associated SAR spectrum is 4 times lower than the one observed by the SAR. The SPRA scheme reproduces the observed SAR spectrum with a swell peak that has a much narrower angular distribution than that of the WAM model. In this way it is able to match the peak value measured by the SAR with a swell system that has only a marginally larger wave height than the one from WAM. The MPIM scheme, however, does not have the option to narrow the angular distribution. To match the observed SAR signal, it has no choice but to increase the energy level in the swell peak significantly.

5.4. Spectral Gap in SPRA Retrievals

Even under light wind conditions, when the azimuthal resolution is not degraded by smearing, the SAR does not resolve waves shorter than 100 m. Hence the SPRA scheme, which relies completely on the SAR for waves other than the parameterized wind sea, is unable to capture swell wave components shorter than 100 m. This is well illustrated in Figure 8. Although the main purpose of the inversion is to retrieve the low-frequency (observed) wave components, there are two reasons why it would be useful to have a better estimate for the higher-frequency components. First, a complete spectrum is much easier to use in applications like wave climate assessment. Second, the higher-frequency components influence the SAR mapping of the longer-wave components through the nonlinear transformation; hence a better estimate of these components may improve the retrieval of the low-frequency components as well. However, this could only be accomplished by adding wave model data to the SPRA inversion scheme. As a side effect, the 180° ambiguity in the swell propagation direction could be removed.

6. Conclusions

The most important conclusion of this validation study is that the MPIM scheme deteriorates the quality of the WAM spectra that it uses as a first guess. Apart from adding a significant bias, the MPIM scheme increases the standard deviation of the significant wave height by more than 30%; for wave components longer than 200 m this increase is 15%. The analysis of the correlations of the errors in the long-wave height H_{12} indicates that the error in the MPIM scheme is largely independent from that of its WAM first guess. The SPRA retrieval scheme performs better than the MPIM scheme, with an accuracy comparable to WAM model output for the wave components longer than 200 m.

Some cases highlight the deficiencies of both schemes. To improve the performance of the MPIM scheme, it is suggested that more physical consistency should be imposed on the wind sea retrieval. Also, evidence is presented that the use of the quasi-linear model in the retrieval may lead to nonlinear features in the SAR spectrum caused by the wind sea to be interpreted as swell. Finally, allowing the spectral width of the WAM partitions to be adapted in the inversion could lead to more sharply peaked SAR spectra, which would be a better match to the observed spectra. To further increase the performance of the SPRA scheme, it seems necessary to add extra first-guess information on the high-frequency wave components, e.g., from a wave model. This would also allow the removal of the 180° ambiguity in the swell retrievals from the SPRA scheme.

SAR data are available on a global scale and therefore may be of considerable value for the specification of the initial condition of global wave models. On the basis of the present validation study, it is clear, however, that to obtain optimal benefits of SAR data for wave analysis, corrections to the MPIM SAR inversion scheme are required. As an alternative, one may contemplate use of the SPRA retrieval scheme, using first-guess wave model spectra.

Acknowledgments. The research was supported by the Netherlands Remote Sensing Board BCRS in the framework of the SPEAR project (contract 1.1/AP-06). The authors would like to thank Patrick Heimbach for making available early results of the MPIM retrieval scheme.

References

Bauer, E., and P. Heimbach, Annual validation of significant wave height of ERS-1 synthetic aperture radar wave mode spectra using TOPEX/Poseidon and ERS-1 altimeter data, *J. Geophys. Res.*, *104*, 13,345–13,357, 1999.

Bauer, E., and C. Staabs, Statistical properties of global significant wave heights and their use for validation, *J. Geophys. Res.*, *103*, 1153–1166, 1998.

Bauer, E., S. Hasselmann, P. Lionello, and K. Hasselmann, Comparison of assimilation results from an optimal interpolation and the Green's function method using ERS-1 SAR wave model spectra, in *Proceedings of the Third ERS Scientific Symposium, Eur. Space Agency Spec. Publ.*, ESA SP414, 1131–1136, 1997.

Breivik, L.-A., M. Reistad, H. Schyberg, J. Sunde, H. E. Krogstad, and H. Johnsen, Assimilation of ERS SAR wave spectra in an operational wave model, *J. Geophys. Res.*, *103*, 7887–7900, 1998.

Donelan, M. A., J. Hamilton, and W. H. Hui, Directional spectra of wind generated waves, *Philos. Trans. R. Soc. London, Ser. A, 315*, 509–562, 1985.

Dunlap, E. M., R. B. Olsen, L. Wilson, S. De Margerie, and R. Lalbeharry, The effect of assimilating ERS-1 fast delivery wave data into the North Atlantic WAM model, *J. Geophys. Res.*, *103*, 7901–7915, 1998.

Engen, G., and H. Johnsen, Sar ocean wave inversion using image cross spectra, *IEEE Trans. Geosci. Remote Sens.*, *33*, 1047–1056, 1995.

Hasselmann, K., and S. Hasselmann, On the nonlinear mapping of an ocean wave spectrum into a SAR image spectrum and its inversion, *J. Geophys. Res.*, *96*, 10,713–10,729, 1991.

Hasselmann, S., C. Brüning, K. Hasselmann, and P. Heimbach, An improved algorithm for the retrieval of ocean wave spectra from synthetic aperture radar image spectra, *J. Geophys. Res.*, *101*, 16,615–16,629, 1996.

Hasselmann, S., P. Lionello, and K. Hasselmann, An optimal interpolation scheme for the assimilation of spectral wave data, *J. Geophys. Res.*, *102*, 15,823–15,836, 1997.

Hasselmann, S., P. Heimbach, and C. Bennefeld, The WASAR algorithm for retrieving ocean wave spectra from SAR image spectra, *Tech. Rep. 14*, 45 pp., Dtsch. Klimarechenzentrum, Hamburg, Germany, 1998.

Heimbach, P., S. Hasselmann, and K. Hasselmann, Statistical analysis and intercomparison of WAM model data with global ERS-1 SAR wave mode spectral retrievals over 3 years, *J. Geophys. Res.*, *103*, 7931–7977, 1998.

Janssen, P. A. E. M., B. Hansen, and J. Bidlot, Verification of the ECMWF wave forecasting system against buoy and altimeter data, *ECMWF Tech. Memo. 229*, Eur. Cent. for Medium-Range Weather Foecasts, Reading, England, UK, 1996.

Komen, G. J., L. Cavaleri, M. Donelan, K. Hasselmann, S. Hasselmann, and P. A. E. M. Janssen, *Dynamics and Modelling of Ocean Waves*, Cambridge Univ. Press, New York, 1994.

Krogstad, H.E., A simple derivation of Hasselmann's nonlinear ocean-synthetic aperture radar transform, *J. Geophys. Res.*, *97*, 2421–2425, 1992.

Krogstad, H.E., O. Samset, and P.W. Vachon, Generalizations of the nonlinear ocean-SAR transform and a simplified SAR inversion algorithm, *Atmos. Ocean*, *32*, 61–82, 1994.

Mastenbroek, C., Spectral wave climate data from spaceborne SAR, in *Proceedings of the CEOS Working Group on Calibration and Validation, SAR Subgroup*, pp. 17–25, Eur. Space Res. and Technol. Cent., Noordwijk, Netherlands, 1998.

Mastenbroek, C., and C. F. de Valk, A semiparametric algorithm to retrieve ocean wave spectra from synthetic aperture radar, *J. Geophys. Res.*, *105*, 3497–3516, 2000.

WAMDI Group, The WAM model: A third generation ocean wave prediction model, *J. Phys. Oceanogr.*, *18*, 1775–1810, 1988.

B. Hansen, ECMWF, Shinfield Road, Reading, Berkshire 9AX RG2, United Kingdom.

C. Mastenbroek, Topicus, Brinkgreverweg 184, 7415 CH Deventer, The Netherlands. (mastenbroek@topicus.nl)

A. C Voorrips, Cap Gemini Ernst & Young, P.O. Box 3101, 3502 GC Utrecht, The Netherlands. (Aart.Voorrips@cgey.nl)

(Received December 6, 1999; revised October 27, 2000; accepted November 27, 2000.)